CIHR Canadian Institutes of Health Research
IRSC Instituts de recherche en santé du Canada

Submitted by CIHR
Déposé par les IRSC

Cold Spring Harb Protoc. Author manuscript; available in PMC 2017 February 08.

Published in final edited form as:
Cold Spring Harb Protoc. ; 2016(6): pdb.prot091306. doi:10.1101/pdb.prot091306.

CIHR Author Manuscript
CIHR Author Manuscript
CIHR Author Manuscript

Using Multiple Whole-Cell Recordings to Study Spike-Timing-Dependent Plasticity in Acute Neocortical Slices

Txomin Lalanne[1,2], **Therese Abrahamsson**[1], and **P. Jesper Sjöström**[1,3]

[1]Centre for Research in Neuroscience, Department of Neurology and Neurosurgery, The Research Institute of the McGill University Health Centre, Montreal General Hospital, Montréal, Québec H3G 1A4, Canada

[2]Integrated Program in Neuroscience, McGill University, 3801 University Street, Montreal, Quebec H3A 2B4, Canada

Abstract

This protocol provides a method for quadruple whole-cell recording to study synaptic plasticity of neocortical connections, with a special focus on spike-timing-dependent plasticity (STDP). It also describes how to morphologically identify recorded cells from two-photon laser-scanning microscopy (2PLSM) stacks.

MATERIALS

It is essential that you consult the appropriate Material Safety Data Sheets and your institution's Environmental Health and Safety Office for proper handling of equipment and hazardous materials used in this protocol.

RECIPES: Please see the end of this protocol for recipes indicated by <R>. Additional recipes can be found online at http://cshprotocols.cshlp.org/site/recipes.

Reagents

Acute hippocampal rodent brain slices

For information on our experience with different slice types and preparation methods, see Protocol: **Long-Term Potentiation by Theta-Burst Stimulation using Extracellular Field Potential Recordings in Acute Hippocampal Slices** (Abrahamsson et al. 2016b).

Artificial cerebrospinal fluid (ACSF) for synaptic plasticity studies <R>

Carbogen gas (95% O_2/5% CO_2)

This gas mixture keeps the slices oxygenated and the pH at ~7.4 during recording.

Internal solution for whole-cell recording <R>

---

[3]Correspondence: jesper.sjostrom@mcgill.ca.

Equipment

Anti-vibration air table (e.g., Newport, TMC, Thorlabs)

Borosilicate capillary glass tubing (Harvard Apparatus [G150F-4])

Contrast enhancement (e.g., Luigs and Neumann DGC tube, Scientifica Dodt contrast, or Olympus DIC)

Dodt contrast can also be custom-built from Thorlabs parts.

Data acquisition board (National Instruments [PCI-6229]; see Fig. 1C)

Electrode holders and silver wire (e.g., Harvard Apparatus [2037760664]; see Fig. 1A,B)

Electrode-tracking software (e.g., Scientifica [LinLab], Wavemetrics [Igor Pro], or MathWorks [MATLAB] for custom-written programs)

Electronic manometer (optional; see Step 3)

Faraday cage (e.g., custom-made, Luigs and Neumann, Scientifica)

Inline heater, sensor, and temperature controller (e.g., Scientifica [HPT-2A], Warner Instruments [SH-27B])

IR-sensitive CCD camera (e.g., Watec [WAT902H], TILL Photonics [VX55])

Micromanipulator (e.g., Scientifica [MicroStar; see Fig. 1A], Luigs and Neumann [MLE/MRE 3axes Mini25])

Motorized microscope with XY stage (e.g., Scientifica [SliceScope Pro], Luigs and Neumann [Infrapatch 380])

Oscilloscope (e.g., Tektronix [TDS2024C]; see Fig. 1C), Picotech [3406A/B])

Patch-clamp amplifier (Dagan Corporation [BVC-700A; see Fig. 1C], Molecular Devices [MultiClamp 700B or Axopatch 200B])

Patch-pipette filler (e.g., Advanced Instruments [MF28G67-5], Eppendorf ["microloader," 930001007])

Pipettes (prepared with pipette puller, e.g., Narishige [PC-10], Sutter Instruments [P-97, P-1000], Harvard Apparatus [PMP-102], AutoMate Zeitz DMZ)

Pressure tubing (see Fig. 1A,B)

Recording acquisition software (e.g., Molecular Devices [pClamp], AxoGraph [AxoGraph X]. Wavemetrics [Igor Pro], or MathWorks [MATLAB] for custom-written programs)

Recording chamber

Slice holder (Harvard Apparatus, Warner Instruments, or custom-made from platinum wire with nylon strands held in place by cyanoacrylate glue [see Fig. 1B])

Software for morphological reconstructions (e.g., Neuromantic [http://www.reading.ac.uk/neuromantic/], Neurolucida [MBF Bioscience], Imaris [Bitplane])

Software for morphometry (e.g., L-Measure [http://cng.gmu.edu:8080/Lm/], Fiji [http://fiji.sc/Fiji])

Stabilizing pipette rod holder (Scientifica; see Fig. 1A)

Three-way stopcocks (e.g., Cole-Parmer [EW-30600-23], VWR [89134-220])

Vacuum system or pump (e.g., Charles Austen [Dymax 5], Masterflex [HV7791620], Gilson [Mini-puls 3])

Water immersion objective (Olympus [40×: LUMPLFLN40XW; see Fig. 1B; 60×: LUMPLFLN60XW])

METHOD

Set up the Experiment

1 Prepare ACSF and internal solution and cut the brain slices (see Protocol: Long-Term Potentiation by Theta-Burst Stimulation using Extracellular Field Potential Recordings in Acute Hippocampal Slices [Abrahamsson et al. 2016b] and Davie et al. 2006). Ensure that *A*CSF is circulating in the recording chamber and that the temperature is 31–34°C.

ACSF should circulate at a rate of at least ~1 drop/sec (~2 mL/min).

2 Hold down the slice in the recording chamber (Fig. 1B) with the slice holder. To ensure that layer 5 (L5) pyramidal cells (PCs) were not damaged during dissection, visualize their apical dendrites as far as L1 if possible. Select the cells to patch, keeping in mind that connectivity is highest for cells located closer than 100-μm apart (Holmgren et al. 2003; Perin et al. 2011) and for neurons deep in the slice (Ko et al. 2011).

Cells that appear smooth are usually healthier than those that are of high contrast.

3 Fill pipettes with internal solution and insert them into the electrode holders. Ensure pressure tubing and wires are attached to electrode holders. Clamp pipettes with a rod (Fig. 1A) to stabilize recordings. Apply positive pressure with a 20-mL syringe or by mouth. Close a three-way stopcock to maintain positive pressure.

An electronic manometer attached to the tubing can be helpful in monitoring pipette pressure.

Perform Patch-Clamping

4   Place all four electrodes just above the region of interest in the slice. Null the amplifier offsets and measure pipette resistances. Use a software solution to semiautomatic electrode movements (e.g., the *Follow* function in LinLab software from Scientifica or custom scripts).

> Computer assistance saves time and reduces the risk of damaging pipettes and/or the tissue.

5   Patch the first cell.

    i.   Approach the cell to be patched. Voltage clamp the pipette to 0 mV and apply a −5-mV test pulse running at 30–40 Hz with 50% duty cycle to monitor pipette resistance with an oscilloscope. Verify the positive pressure—as you advance the pipette through the slice, the positive pressure should push tissue aside. Approach the cell slowly, ideally along the diagonal axis of the pipette while circumventing other cells.

> Do not go straight through other cells, as this makes the tip dirty, which makes the formation of a GΩ seal difficult or impossible.

> If the test pulse readout suddenly drops, the tip has become blocked, either by dirt inside the pipette or by brain tissue.

    ii.   When the pipette tip is located ~10 μm from the cell, reduce positive pressure: open the three-way stopcock, then reapply and hold positive pressure quickly by mouth. Advance the pipette tip a few microns into the cell until a dimple forms. Quickly release the pressure and gently apply light negative pressure to gradually form a GΩ seal without rupturing it (see Step 7).

    iii.   As seal resistance increases beyond ~100 MΩ, switch the holding voltage from zero to −70 mV, as this helps establish the GΩ seal. Once the GΩ seal is formed, open the stopcock and release to atmospheric pressure.

6   Repeat Step 5 for the other three electrodes.

> As the next pipette is brought down into the tissue with positive pressure, the tissue moves, thus requiring continual readjustments of the previous electrodes. Ideally, the tip of the pipettes should follow any movement of the cell so that the pipette tip remains at the same position relative to the cell as when it was first patched.

7   Rupture the four patches.

    i.   Once four GΩ seals have been established, go into whole-cell configuration. Doing this in quick succession on all four cells ensures that intracellular components necessary for plasticity induction are not dialyzed unequally from the different cells (Malinow and Tsien 1990; *Sjöström et al. 2001*).

> **ii.** Gradually apply gentle suction until the patch is ruptured while monitoring the oscilloscope test pulse.
>
>> Patch rupture is evidenced by a sudden increase in test pulse current step. The negative pressure ramp may have to be repeated a few times. If the seal does not rupture, try hyperpolarizing the cell to −140 mV until rupture (see Troubleshooting).
>
> **iii.** Switch to current clamp and remove negative pressure.

8 Once broken through, assess quality of whole-cell recordings.

> Typical resting membrane potential and input resistance for visual cortex L5 PCs of postnatal day 14–16 (P14–P16) rats is −65 ± 3.4 mV (mean ± s.d.) and 110 ± 45 MΩ, respectively (n = 325; P.J. Sjöström, unpubl.), although the distribution of the latter parameter has a long tail extending beyond 300 MΩ, and both values vary with age (Sjöström et al. 2001). The series resistance should be as low as possible, but is, as a rule of thumb, not less than double the pipette resistance. In practice, series resistances as high as 20–30 MΩ are satisfactory for plasticity experiments performed in current clamp, but voltage clamp is compromised by high or variable series resistance. A typical P14 visual cortex L5 PC will produce a single spike after a 5-ms 1.3-nA current injection. Spikes should typically be 1–2 msec in width at half height—if broader, the series resistance may be too high, which results in artificial spike broadening by temporal filtering.

Identify Connected Pairs of Neurons

9 Search for connections by evoking spikes in all four cells (Fig. 2A,B, top), staggered by at least 500 msec to avoid accidental STDP induction (Sjöström et al. 2001). Generate spike-triggered averages of 10–40 postsynaptic sweeps to ensure that weak connections are not missed. Verify that connections found are monosynaptic: response latency and temporal jitter should be submilli-second (Fig. 2C,D).

Induce Plasticity

10 Once connections have been identified, start the STDP protocol.

> *First, a baseline period of 10 min or more should be acquired. Next, STDP is elicited by repeated pre- and postsynaptic spike pairings at the desired frequency and timing. A post-pairing period then follows, identical to the baseline but maintained for at least 30 min and ideally longer (Fig. 3A,B). At L5 PC connections, repeated pre-before-postsynaptic spike pairings at a timing difference of t = +10 msec result in potentiation if the frequency or depolarization is high enough, whereas the opposite temporal order may elicit depression (Fig. 3C; Sjöström et al. 2001 bottom).*

Analyze Acquired Data

11   Use a dedicated analysis software program, because data analysis is time consuming and highly repetitive.

> Software can be purchased (e.g., pClamp, or AxoGraph X), but customization (e.g., in Igor Pro or MATLAB) maximizes flexibility and speed. Microsoft Excel is also quite adequate for basic analysis or for part of the analysis.

12   Discard recordings with unstable baseline.

> To avoid bias in the data selection, it is important to apply the same stability criterion to all recordings. One suitable requirement is that the baseline should not change more than, e.g., 10% (Markram et al. 1997). An alternative is to apply a t-test to the differences of the means of the two baseline period halves. A stable baseline is indicated by a nonsignificant P-value. Similarly, a two-tailed t-test of Pearson's r for response amplitude versus time during the baseline period should not be significant, as this would violate the null-hypothesis that baseline responses have no upward or downward trend.

13   Apply quality-control criteria.

> Recordings should consistently be discarded or truncated if the resting membrane potential, perfusion temperature, or input resistance venture outside bounds. The specifics of these bounds are somewhat arbitrary but can be: input resistance should not change >30%, resting membrane potential should not be more than 8 mV, and temperature should remain within 31–34°C (Fig. 3D; Sjöström et al. 2001). In voltage clamp, also monitor series resistance: it should, e.g., be less than 25 MΩ, not change >20%, and/or be indistinguishable from that in the control experiments (Sjöström et al. 2003).

14   Quantify the magnitude of plasticity. Measure plasticity as the change in EPSP amplitude after the induction protocol compared with the amplitude before induction, expressed in percentage terms. Ignore the first several minutes after the induction, as other forms of plasticity may be active during this period, e.g., post-tetanic potentiation (Zucker and Regehr 2002).

> We typically compare the responses starting 10 min after the induction until the end of the recording, to the entire prepairing baseline (Fig. 3C; Sjöström et al. 2001, 2003).

15   Morphologically classify the recorded cells.

> **i.**   Image the entire volume in which recorded neurons arborize (Fig. 4A). Use software such as Neuromantic, Neurolucida, or Imaris to reconstruct neurons from 2PLSM image stacks (Blackman et al. 2014), carefully distinguishing dendrites from axons by the presence of dendritic spines characteristic of neocortical pyramidal cells (Fig. 4B).

> L-Measure provides useful numerical morphometry measurements
> (Scorcioni et al. 2008).

ii. To obtain ensemble averages, create arbor density maps (Buchanan et
al. 2012) (Fig. 4C) or carry out Sholl analysis (Fig. 4D; Sholl and
Uttley 1953).

> To save time, Scholl analysis can be directly performed on bitmap
> images using Fiji (Ferreira et al. 2014).

16 Repeat experiments. To produce a complete STDP curve or to examine the rate
dependence of plasticity, repeat experiments in different paired recordings with
similar cell types while varying the timing (e.g., −120 msec to +40 msec) or rate
(e.g., 0.1 Hz to 60 Hz) during the induction (Sjöström et al. 2001).

> It is generally not appropriate to repeat different inductions in sequence in
> the same connected pair, because depression of previously potentiated
> synapses is not necessarily the same as depressing a naïve connection
> (Massey and Bashir 2007).

TROUBLESHOOTING

Problem: Seals and recordings are of poor quality

Solution:

1 Pipette resistance has to be in the right range. Seals form more easily with high
pipette resistance (4–6 MΩ), although as a consequence, it may be harder to
rupture the patch, and the resulting series resistance will be higher. If the patch
does not rupture when applying negative pressure, try hyperpolarizing the cell to
−140 mV until membrane rupture. With this approach, be ready to quickly
switch from voltage to current clamp as soon as whole-cell mode is established,
to avoid damaging the cell with the large negative current that results from
clamping it to −140 mV. With a GΩ seal that resists rupture even at this point,
you can try more aggressive tricks such as applying large negative pressure with
a 20-mL syringe, or using the amplifier's "buzz" function. These tricks,
however, are rarely successful, but represent a last resort. With lower pipette
resistance (3–4 MΩ), the pipette tip will be larger, so the series resistance will be
lower, but sealing may be more difficult. Once a seal has been established,
breaking through to go whole-cell is easier, however. The use of large pipette
tips with low pipette resistance is thus recommended for voltage clamp
experiments. For quadruple whole-cell recordings in current clamp, however, it
is typically more important to establish good seals with high success rate on all
four cells, because failure to record from one out of the four cells reduces the
number of tested connections from 12 to 6—a 50% reduction in yield of
connections.

2 Pipette tips may be dirty. Remove visible debris with large positive pressure
using a 50-mL syringe. If this fails, change the pipette—patching with dirty tips

is rarely successful. To reduce clogging of the pipette from the inside, always filter the internal solution with a nylon syringe filter (0.2 μm, e.g., Nalgene #176). Sonicating the filling solution before use may also help.

3   Pressure may be too low. Leaky pressure lines should be replaced. Apply positive pressure before the pipette enters the ACSF. In the absence of positive pressure, debris tends to stick to the pipette tip, making patching much more difficult.

4   External/internal solutions may not be optimal. The difference in internal and external solution osmolality determines the ease of patching. For rat slices, internal osmolality should be ~294 mOsm (adjusted with sucrose), whereas the ACSF should be ~320 mOsm (adjusted with D-glucose). For mouse slices, osmolalities should be 17 mOsm higher (Bourque 2008).

5   Animal age may not be optimal. For rat slices, P13–P16 is the ideal age, whereas for mice it is 1–2 days younger. Although cell health is often inferior in slices from older animals, cells might not have acquired mature properties in slices from young animals. With older animals, cardiac perfusion or high-sucrose dissection solution may improve slice quality (Moyer and Brown 1998).

6   Slice quality may have deteriorated. Replace the slice with a new one, or dissect a new animal. Slices generally decline faster at 31–34°C than at room temperature. In P14 rat slices may be usable up to 10 h after dissection, whereas P18 slices may last no more than 5 h. Slices from mouse brain deteriorate faster than rat slices do.

Problem: Connected pairs of neurons cannot be found

Solution:

7   The slice may not have been cut at an optimal angle. A slice with L5 PC apical dendrites reaching layer 1 is likely to have well-preserved connectivity.

8   Patch cells deeper into the slice. Although visibility and rate of successful patching drop below 80 μm, there are returns in terms of higher connectivity rates (Ko et al. 2011). A reasonable tradeoff is to patch 50–80 μm deep.

9   Use a train of presynaptic spikes and average more sweeps to better visualize weak postsynaptic responses and synapses with low release probability.

Problem: Electrical problems with recordings

Solution:

10   Recordings may be noisy. Make sure headstages and bath chamber are grounded. Do not ground the same device several times, as this creates ground loops and possibly results in more noise. Ground all devices to the same grounding point to minimize grounding loops. Noisy devices should be disconnected, substituted, or moved farther away.

11 Voltages may slowly drift because of slow polarization of electrodes. To slow down voltage drift, increase electrode surface area by covering electrodes in chloride. Leave them in bleach (sodium hypochlorite or hydrogen peroxide) for 10 min. Alternatively, pass a positive current through the electrode dipped in 1 M NaCl using, for example, a 4.5-V battery until a white layer appears.

12 Series resistance may be too high. The GΩ seal may not have been completely ruptured. Apply a light negative pressure. If the problem persists, use pipettes with larger tip diameter.

Problem: Recordings are not stable

Solution:

13 Prepare new intra and/or extracellular solutions.

14 The slice may not have been cut in the right orientation, and therefore recorded cells are damaged. Pick a new slice from the incubation chamber. Flipping the slice over in the chamber and recording from the other side may also help.

15 Baseline stimulation frequency may be too high, hence the synapse may not have enough time to recover from short-term depression. For single EPSPs, use an inter-stimulus interval of 7–10 sec. A train of five EPSPs at 30–50 Hz requires 15–18 sec for full recovery (Varela et al. 1997; Buchanan et al. 2012).

16 Verify that the perfusion temperature is stable and set correctly. Temperature variations cause fluctuations in EPSP amplitude and passive properties. Deterioration can be very rapid at 37°C.

Problem: It is difficult to obtain long-term potentiation (LTP) or long-term depression (LTD)

Solution:

17 Baseline longer than 15 min may result in plasticity washout (Malinow and Tsien 1990).

18 Verify that both pre- and postsynaptic cells spike during the induction.

19 Average across five to eight paired recordings; do not make too much of the outcome of individual connections.

DISCUSSION

Compared with field recordings, the quadruple patch-clamping technique is expensive to set up and more challenging to master. It does, however, have several advantages such as millisecond temporal precision, specific pharmacological access to pre- and postsynaptic cells, and morphological identification of connected cells. For additional background on both methods, see **Introduction: In Vitro Investigation of Synaptic Plasticity** (Abrahamsson et al. 2016a).

With multiple whole-cell recordings, the statistics of local connections can also be studied. For example, neocortical pyramidal cells are reciprocally connected to a greater degree than expected from a uniformly random distribution (Song et al. 2005). This may result from Hebbian plasticity, so that cells coding for similar information are wired together more strongly (Ko et al. 2011). The juvenile cerebellar Purkinje cell network, on the other hand, is solely built from chains of unidirectionally connected neurons (Watt et al. 2009). This forms a substrate for travelling waves of activity, which may help wire the circuit up in early development (van Welie et al. 2011). Quadruple recordings provide an excellent means of assessing such network-specific differences in patterns of connectivity.

Multiple whole-cell recordings do represent a financial hurdle, however. A less expensive alternative is to search for presynaptic cells using loose patch while whole-cell recording the postsynaptic cell (Feldmeyer et al. 1999; Barbour and Isope 2000). Unfortunately, this approach has the disadvantage that it may subject the postsynaptic cell to plasticity washout (Malinow and Tsien 1990).

In the end, multiple whole-cell recording is technically similar to patching single cells. With this protocol, an experimentalist capable of reliably patching individual cells should not find quadruple whole-cell recordings too challenging.

RECIPES

Artificial Cerebrospinal Fluid (ACSF) for Synaptic Plasticity Studies

Prepare the following 10× stock solution in double-distilled water (ddH$_2$O). Store it at 4°C for a maximum of 1 wk.

Compound	Concentration of 10× stock
NaCl	1250 mM
KCl	25 mM
NaH$_2$PO$_4$	12.5 mM
NaHCO$_3$	260 mM

On the day of the experiment, dilute the 10× solution 10-fold, bubble for 10 min with carbogen (95% O$_2$/5% CO$_2$), and supplement with the following. (artificial cerebrospinal fluid [ACSF]—in particular Ca^{2+} and Mg^{2+} concentrations—may be varied depending on what is to be studied. For example, higher Ca^{2+} concentration favors long-term potentiation [LTP] whereas lower Ca^{2+} concentration promotes long-term depression [LTD].) Adjust osmolality to ~320 mOsm with D-glucose for rat and ~338 mOsm for mouse.

Compound	Final concentration
MgCl$_2$	1 mM
CaCl$_2$	2 mM

Compound	Final concentration
Glucose	~26 mM

Internal Solution for Whole-Cell Recording

Prepare a 1 M solution of HEPES in ddH$_2$O and adjust the pH to 7 with 3 M KOH. Then prepare 30 mL of the following solution in ddH$_2$O. Adjust the volume to 45 mL and verify that pH ~7.

Compound	Final concentration in 50 mL
KCl	125 mM
K Gluconate	2.5 mM
HEPES (1 M, pH 7)	10 mM

To the previous solution, add the following. Readjust the pH to 7.2–7.4 with KOH and correct the osmolality to 294 mOsm (rat) or 311 mOsm (mouse) with sucrose.

Compound	Final concentration in 50 mL
MgATP	4 mM
NaGTP	0.3 mM
Na-Phosphocreatine	10 mM

Filter the solution using a nylon filter (pore size 0.2 μm, e.g., Nalgene #176) and make 1-mL aliquots. Store at −20°C for up to 6 mo. Verify the osmolality when thawed.

Acknowledgments

References

Abrahamsson T, Lalanne T, Watt AJ, Sjöström PJ. In vitro investigation of synaptic plasticity. Cold Spring Harb Protoc. 2016a; doi: 10.1101/pdb.top087262

Abrahamsson T, Lalanne T, Watt AJ, Sjöström PJ. Long-term potentiation by theta-burst stimulation using extracellular field potential recordings in acute hippocampal slices. Cold Spring Harb Protoc. 2016b; doi: 10.1101/pdb.prot091298

Barbour B, Isope P. Combining loose cell-attached stimulation and recording. J Neurosci Methods. 2000; 103:199–208. [PubMed: 11084213]

Blackman AV, Grabuschnig S, Legenstein R, Sjöström PJ. A comparison of manual neuronal reconstruction from biocytin histology or 2-photon imaging: morphometry and computer modeling. Front Neuroanat. 2014; 8:65. [PubMed: 25071470]

Bourque CW. Central mechanisms of osmosensation and systemic osmoregulation. Nat Rev Neurosci. 2008; 9:519–531. [PubMed: 18509340]

Buchanan KA, Blackman AV, Moreau AW, Elgar D, Costa RP, Lalanne T, Tudor Jones AA, Oyrer J, Sjöström PJ. Target-specific expression of presynaptic NMDA receptors in neocortical microcircuits. Neuron. 2012; 75:451–466. [PubMed: 22884329]

Costa RP, Sjöström PJ, van Rossum MCW. Probabilistic inference of short-term synaptic plasticity in neocortical microcircuits. Front Comput Neurosci. 2013:7. [PubMed: 23444270]

Davie JT, Kole MH, Letzkus JJ, Rancz EA, Spruston N, Stuart GJ, Hausser M. Dendritic patch-clamp recording. Nat protoc. 2006; 1:1235–1247. [PubMed: 17406407]

Feldmeyer D, Egger V, Lübke J, Sakmann B. Reliable synaptic connections between pairs of excitatory layer 4 neurones within a single 'barrel' of developing rat somatosensory cortex. J Physiol. 1999; 521(Pt 1):169–190. [PubMed: 10562343]

Ferreira TA, Blackman AV, Oyrer J, Jayabal S, Chung AJ, Watt AJ, Sjostrom PJ, van Meyel DJ. Neuronal morphometry directly from bitmap images. Nat methods. 2014; 11:982–984. [PubMed: 25264773]

Holmgren C, Harkany T, Svennenfors B, Zilberter Y. Pyramidal cell communication within local networks in layer 2/3 of rat neocortex. J Physiol. 2003; 551:139–153. [PubMed: 12813147]

Ko H, Hofer SB, Pichler B, Buchanan KA, Sjöström PJ, Mrsic-Flogel TD. Functional specificity of local synaptic connections in neocortical networks. Nature. 2011; 473:87–91. [PubMed: 21478872]

Malinow R, Tsien RW. Presynaptic enhancement shown by whole-cell recordings of long-term potentiation in hippocampal slices. Nature. 1990; 346:177–180. [PubMed: 2164158]

Markram H, Lübke J, Frotscher M, Sakmann B. Regulation of synaptic efficacy by coincidence of postsynaptic APs and EPSPs. Science. 1997; 275:213–215. [PubMed: 8985014]

Massey PV, Bashir ZI. Long-term depression: multiple forms and implications for brain function. Trends Neurosci. 2007; 30:176–184. [PubMed: 17335914]

Moyer JR Jr, Brown TH. Methods for whole-cell recording from visually preselected neurons of perirhinal cortex in brain slices from young and aging rats. J Neurosci Methods. 1998; 86:35–54. [PubMed: 9894784]

Perin R, Berger TK, Markram H. A synaptic organizing principle for cortical neuronal groups. Proc Natl Acad Sci. 2011; 108:5419–5424. [PubMed: 21383177]

Scorcioni R, Polavaram S, Ascoli GA. L-Measure: a web-accessible tool for the analysis, comparison and search of digital reconstructions of neuronal morphologies. Nat protoc. 2008; 3:866–876. [PubMed: 18451794]

Sholl A, Uttley AM. Pattern discrimination and the visual cortex. Nature. 1953; 171:387–388. [PubMed: 13036904]

Sjöström PJ, Turrigiano GG, Nelson SB. Rate, timing, and cooperativity jointly determine cortical synaptic plasticity. Neuron. 2001; 32:1149–1164. [PubMed: 11754844]

Sjöström PJ, Turrigiano GG, Nelson SB. Neocortical LTD via coincident activation of presynaptic NMDA and cannabinoid receptors. Neuron. 2003; 39:641–654. [PubMed: 12925278]

Song S, Sjöström PJ, Reigl M, Nelson S, Chklovskii DB. Highly non-random features of synaptic connectivity in local cortical circuits. PLoS Biol. 2005; 3:e68. [PubMed: 15737062]

van Welie I, Smith IT, Watt AJ. The metamorphosis of the developing cerebellar microcircuit. Curr Opin Neurobiol. 2011; 21:245–253. [PubMed: 21353528]

Varela JA, Sen K, Gibson J, Fost J, Abbott LF, Nelson SB. A quantitative description of short-term plasticity at excitatory synapses in layer 2/3 of rat primary visual cortex. J Neurosci. 1997; 17:7926–7940. [PubMed: 9315911]

Watt AJ, Cuntz H, Mori M, Nusser Z, Sjöström PJ, Häusser M. Traveling waves in developing cerebellar cortex mediated by asymmetrical Purkinje cell connectivity. Nat Neurosci. 2009; 12:463–473. [PubMed: 19287389]

Zucker RS, Regehr WG. Short-term synaptic plasticity. Annu Rev Physiol. 2002; 64:355–405. [PubMed: 11826273]
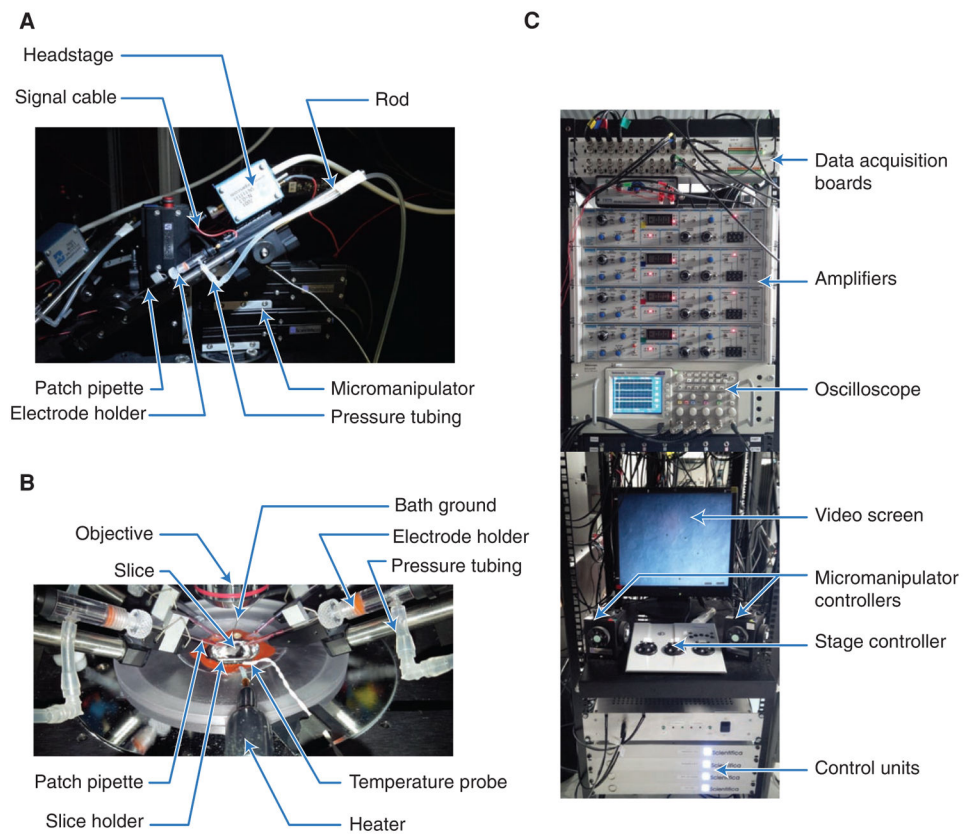
FIGURE 1.
Recording setup. (*A*) Motorized micromanipulator with patch pipette. With this design, the rod is slid away from the chamber for pipette exchange; other designs may rotate or swing backward. The mode of pipette exchange determines the total number of manipulators that can be fit. (*B*) Perfusion chamber during quadruple whole-cell recording. Pipettes are filled with enough internal solution to touch the electrode wire. Glass pipettes are clamped to the rod to minimize movements. The temperature probe and the bath ground should be fully immersed in ACSF. (*C*) Acquisition boards provide communication between computer and amplifiers. Recording channels and manipulators are color-coded (see oscilloscope screen) for simplicity. Video screen shows a Dodt-contrast-enhanced image of the slice. Microscope stage, objective, and manipulators are remotely controlled to minimize the risk of disrupting ongoing recordings.
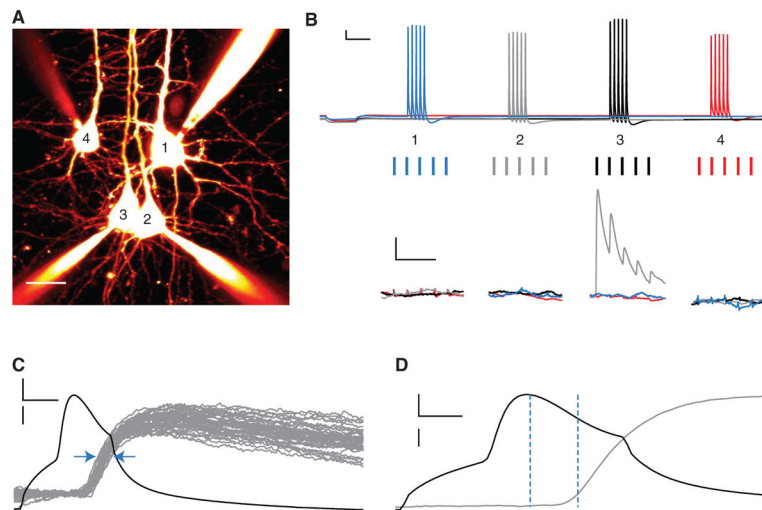
FIGURE 2.

Finding connected neurons using quadruple recordings. (*A*) Flattened two-photon-imaging stack of four neighboring L5 PCs filled with Alexa 594 (scale bar: 25 μm). (*B*) Thirty Hertz trains are evoked (*top*, scale bars: 200 msec, 10 mV) to identify responding postsynaptic cells (*bottom*, scale bars: 100 msec, 0.25 mV). Sweeps should be repeated 10–40 times every 10–20 sec, and are then averaged. Note short-term depressing connection from cell 3 (black) to cell 2 (gray). (*C*) Monosynaptic connections have a jitter of less than 1 msec (blue arrows); larger jitter suggests that the responses are polysynaptic. Fifty spike-triggered traces (gray) from cell 2 are represented, whereas the presynaptic action potential (black) is represented by a single sweep (scale bars: 2 msec, 20 mV [black]/300 μV [gray]). (*D*) Monosynaptic connections also have submillisecond latency between presynaptic spike and 10% of EPSP peak (vertical dashed lines). EPSP trace (gray) is a spike-triggered average of 50 sweeps, whereas the presynaptic action potential (black) is represented by a single sweep (scale bars: 1 msec, 20 mV [black]/200 μV [gray]).
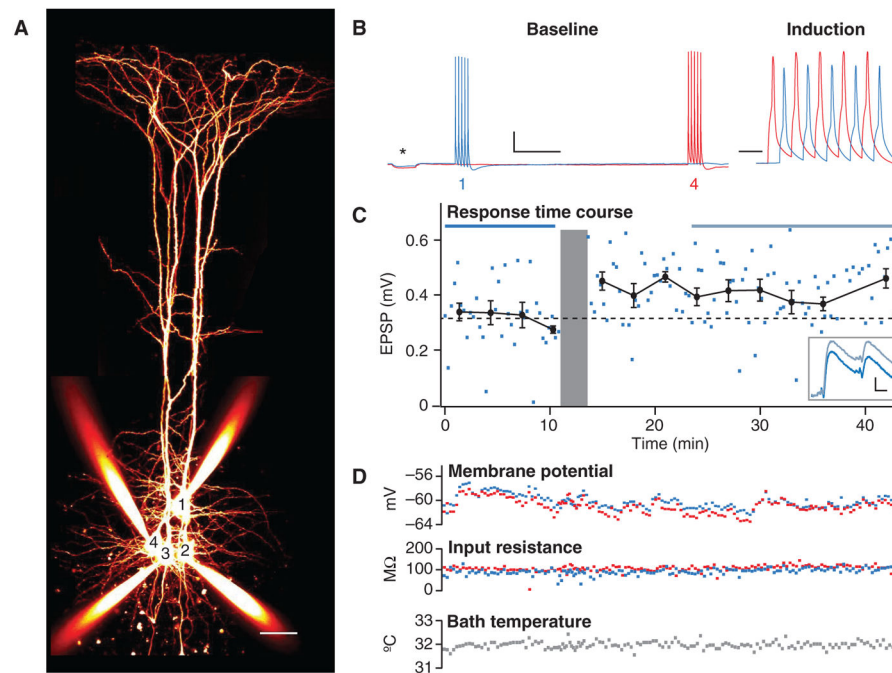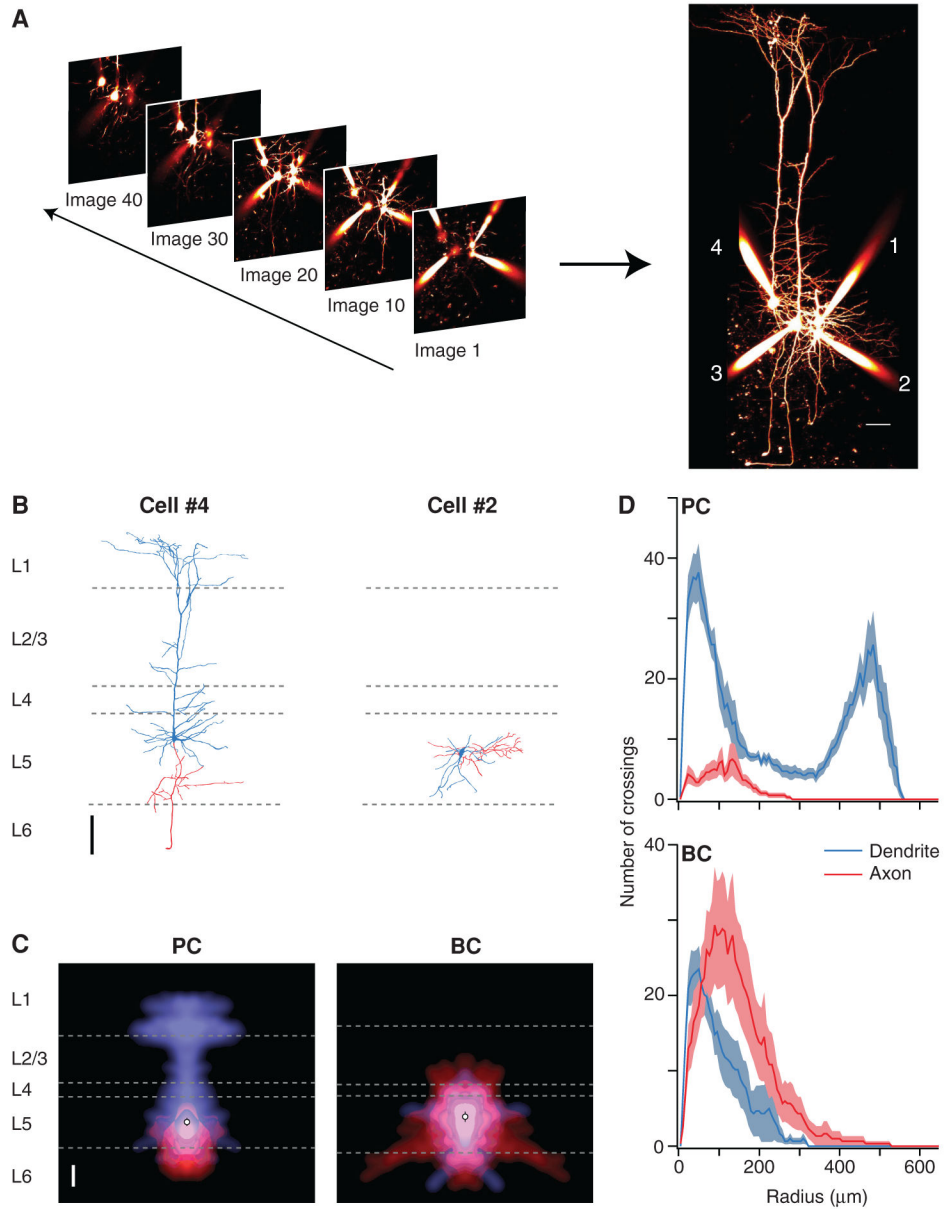
FIGURE 3.

Using paired recordings to study plasticity. (*A*) Quadruple whole-cell recording in which PC 4 was connected to PC 1 (scale bar: 50 μm). (*B*) During the 10-min baseline period, 30-Hz trains were repeated every 18 sec in the connected pair of neurons. These bursts were separated by long intervals to avoid induction of long-term plasticity (Sjöström et al. 2001). During the induction, 5 action potentials at 50 Hz were repeated 15 times every 15 sec. The timing difference was +10 msec. After the induction, the baseline pattern was resumed (scale bars: 500 msec [baseline]/20 msec [induction], 20 mV). Asterisk denotes a 250-ms test pulse of −50 pA, used to monitor input resistance. (*C*) Time course of the first EPSP in the 30-Hz train shows LTP. The induction is illustrated by the gray area. Horizontal blue lines (top) represent time periods over which averages (inset) were taken (scale bars: 10 msec, 0.1 mV). Using such averaged traces, measuring changes in short-term plasticity (Costa et al. 2013) can be used to assess the locus of plasticity expression (Sjöström et al. 2003). (*D*) As a measure of recording quality, resting membrane potential, input resistance, and bath temperature were monitored throughout experiment. Blue and red indicate cell 1 and cell 4, respectively.

FIGURE 4.

Morphological cell classification from two-photon images. (*A*) A stack of two-photon slices provides a 3D representation of recorded neurons filled with Alexa 594. Each slice is an average of two to four 512×512-pixel frames collected. Maximum-intensity projections are assembled for full morphological view (scale bar: 50 μm). (*B*) Digital reconstruction of cell 4 (left) shows that this is a neocortical L5 pyramidal cell (PC), whereas the morphology of cell 2 (right) is characteristic of a basket cell (BC; scale bar: 100 μm). Reconstructions were performed using Neuromantic (Blackman et al. 2014). Dendrites (blue) and axons (red) were distinguished by the presence of dendritic spines or axonal boutons. Dashed gray lines represent layer boundaries, as determined from simultaneously acquired laser-scanning Dodt contrast images. (*C*) Morphology density map (Buchanan et al. 2012) of six PCs (left)

highlights the characteristic apical dendrite, with an axonal arborization that remains localized to L5. The corresponding map of six BCs (right) shows axonal and dendritic arbors that both remain confined to L5. Average soma location indicated by open circle (scale bar: 100 μm). (*D*) Sholl Analysis (Sholl and Uttley 1953) of six PCs (*top*) and six BCs (*bottom*) provides quantitative cell classification criteria from axonal and dendritic branching patterns.